Proceedings of the ASME 2017 Pressure Vessels & Piping Division Conference
PVP2017
July 16-20, 2017, Waikoloa, Hawaii, United States

PVP2017-65404

SURFACE ROUGHNESS 3D MODELLING AND ITS ASSOCIATION WITH LEAK TIGHTNESS FOR A METAL-TO-METAL CONTACTING SURFACE

Ali A. Anwar*
WEIR Advanced Research Centre
Mechanical and Aerospace Engineering
University of Strathclyde
Technology and Innovation Centre
99 George St, Glasgow, G1 1RD
ali.anwar@strath.ac.uk

William Dempster
Yevgen Gorash
David Nash

Mechanical and Aerospace Engineering
University of Strathclyde,
James Weir Building
75 Montrose St, Glasgow, G1 1XJ
william.dempster@strath.ac.uk
yevgen.gorash@strath.ac.uk,

ABSTRACT

This paper presents an overview of a numerical method developed to allow one-way structure-fluid interaction of a scanned representative surface of a Pressure Relief Valve (PRV) measuring 100 μm by 100 μm to be incorporated into a coupled finite element and computational fluid dynamics model to investigate gas leak rates through micro-gaps in full size metal-to-metal contacting components. The virtual representative surface is created via a real scan using a 3D micro coordinate and surface roughness measurement system. The scan of the physical surface is converted to a CAD format and a finite element model generated which is deformed for a given loading condition. The micro-gaps of the deformed FEA model are extracted and imported into the CFD solver to find the resulting volumetric/mass flow rate for the same set of pressure conditions. This coupled approach allows the leakage rate to be found based on only the surface roughness of metal-to-metal sealing surfaces. This methodology can now be expanded to understand the behaviour and response of metal-to-metal deformable contacting surface components under pressure. Thereafter, the design objective is to minimise or eliminate component leakage.

NOMENCLATURE

A_{eff}	effective fisc area
$F_{local\ spring}$	local spring force
Kn	Knudsen Number
L	channel length
P_{in}	inlet pressure
P_{out}	outlet pressure
P_{set}	set pressure
R_a	average roughness
R_{in}	inner radius of seat
R_{out}	outer radius of seat
R_{sm}	average roughness spacing between peaks/valleys
W_a	average waviness
W_{sm}	average waviness spacing between peaks/valleys

INTRODUCTION

The role a Pressure Relief Valve (PRV) plays in a pressurised system is simple, yet from a safety perspective, arguably the most important. PRV's are commonly used in nuclear power plants for both the primary and secondary reactor coolant systems. The role it plays is to relieve the system of over-pressure; maintaining the pressurised system at a safe level.

A PRV's design has not changed very much since its origin. A known issue with metal-to-metal seal PRV's is leakage which subsequently can cause set-pressure (P_{set}) drift. This issue can have a detrimental widespread outcome such as the incident which occurred in 2013 with the US Pilgrim Nuclear Power station. It was reported that 3 of the 4 Pilot Operated PRV's were

*Address all correspondence to this author.

leaking in the primary coolant cycle which forced the power station to shut-down [1].

Japan's Atomic Energy Agency (JAEA) reviewed the trend of incidents of US power stations (years 2000 to 2006), finding the second dominant cause of set-pressure drift of PRV's being leakage [2].

PRV leak tightness guarantee provided by both manufacturers and consumers is of great importance. A consumer would want to ensure the leak tightness is guaranteed to safeguard working conditions. Manufacturers guarantee leak tightness by complying with standards such as *API 527:Seat Tightness of Pressure Relief Valves* [3] and dependant on region the equivalent standard would be used i.e. *British Standard-BS EN ISO 4126-1:2013* [4]; *ASME Standard-ASME PTC 25-2014* [5], etc. When in operation, as a PRV reaches its set-pressure the leakage rate increases. Therefore, having the ability to design according to standards and reduce the leakage of a PRV allows valve manufacturers to create a market competitive product.

In the past, organisations such as the Midwest Research Institute (on behalf of NASA) [6] and the European Commission Community Research [7] attempted to understand: why valve leakage occurs; the underlying physics to predict leakage; and monitoring/assessing leakage. To date overall research directly relating to metal-to-metal contact PRV leakage is scarce.

Nonetheless, understanding of PRV leakage can be drawn from relevant fields such as: metal-to-metal contact and gasket seals. When these metal surfaces come into contact in parallel to each other a finite gap or path is present which is dictated by key metrology surface finish quality such as: form; waviness; and roughness. Subsequently, if there is a driving internal pressure the fluid can navigate through the path and exit the valve resulting in leakage [8].

In this paper, a new numerical modelling method is presented to model metal-to-metal contact leakage of PRV's based on the surface roughness only. The metal-to-metal contact surfaces of a PRV are the 'Seat' and 'Disc' (see Fig. 1). This method relies upon measuring the fine key metrology characteristics of both these 'poli-lapped' surfaces. The surface finish characteristic, roughness, is represented using a 100 μm by 100 μm scan discretised geometric model. This geometric model is numerically analysed using Finite Element Analysis (FEA) to understand the effect on the finite gap due to the spring force. The resultant gap is exported and assuming laminar gas micro-flow (ranging from the slip flow to the continuum flow regime) a Computational Fluid Dynamics (CFD) solver is used to find the leakage associated to the roughness.

The PRV of interest for this research is spring-loaded with a 19.25 mm internal radius. Using the new numerical modelling method, leakage of the Seat-Disc contact up to a set-pressure of 0.5 MPa are presented. The results of leakage based on surface roughness contact per 100 μm width are presented, discussed and concluded.

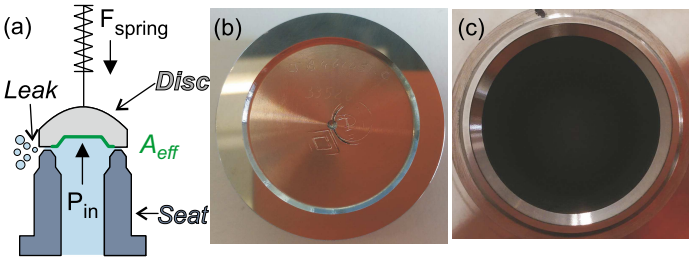

FIG. 1 (a) SIMPLE DIAGRAM OF PRV WITH SPRING FORCE (F_{spring}), INTERNAL PRESSURE (P_{in}), SEAT, DISC AND EFFECTIVE DISC AREA (A_{eff}) HIGHLIGHTED (b) DISC (BOTTOM VIEW) (c) SEAT (TOP VIEW)

VALVE LEAK TIGHTNESS METHODOLOGY

Within a PRV, a compressed spring applies a force on the disc which is transferred to the seat due to the metal-to-metal contact. As the internal pressure (P_{in}) of the fluid increases, the overall force on the disc and seat decreases, until eventually the pressure reaches (P_{set}) exceeding the force of the spring, pushing the Disc off of the Seat and opening the valve. When the Disc and Seat are in contact, there is leakage of fluid between the Seat and Disc. Therefore, an investigation of the metrology characteristics of the contacting surfaces is required to determine: the finite gap this creates between the Seat and Disc; how the spring force (F_{spring}) deforms the finite gap; and ultimately how much fluid passes through the gap.

This numerical method is split up into 4 sections: Metrology; Computer Aided Design (CAD); FEA; and CFD. By finding first the metrology characteristics of the contacting surface, a CAD model can be created and independently analysed to find the effect of the spring force on the metallic contact surfaces and subsequently the finite gap. The deformed gap between the contacting surfaces in the FEA analysis is exported into a CFD solver allowing analysis of the fluid flow through the gap finding the leakage. A breakdown of the sections and the two models is represented in a flow diagram in Fig. 2.

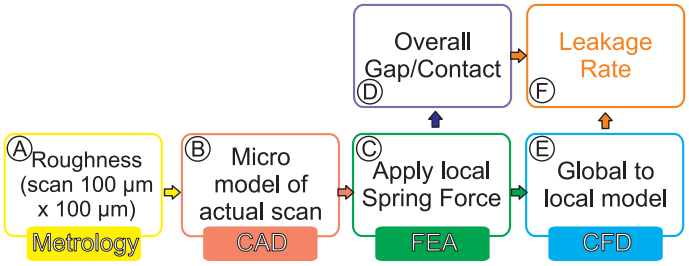

FIG. 2 VALVE LEAK TIGHTNESS METHODOLOGY FLOW DIAGRAM

Metrology

As mentioned, when the disc and seat are in contact, there is a leakage of fluid between the seat and disc. This leakage is associated with a finite gap between the seat and disc contacting surfaces. In turn, the finite gap is a formation of the surface finish quality of the seat-disc contact. Both the seat and disc contact surfaces are 'poli-lapped' i.e. polished and lapped simultaneously, to produce a mirror finish appearance (see Fig. 1), giving the appearance that the surface is 'smooth' or 'flat'; closer examination reveals otherwise.

The metrology features which require examination to understand the extent of the gap are: average surface form; average waviness (W_a, W_{sm}); and average roughness (R_a). What and how these surface features are interlinked is displayed in Fig. 3, which shows the roughness being a sub-feature of the waviness, and the waviness being a sub-feature of the form.

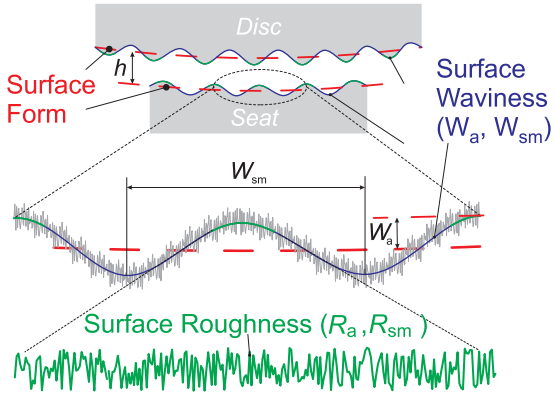

FIG. 3 METROLOGY CHARACTERISTICS: AVERAGE SURFACE FORM; AVERAGE WAVINESS; AND ROUGHNESS

Using a non-contact optical interferometry device the surfaces are examined more closely to reveal the true surface finish quality. The interferometry device used for this paper was an Alicona InfiniteFocus. The mean form deviation (flatness), the waviness and roughness characteristics are presented in Table 1.

	Mean Form deviation (Flatness) (μm)	W_a (W_{sm}) (μm)	R_a (μm)
Disc	4.38	0.21 (1751)	0.041
Seat	2.1	0.11 (2449)	0.068

TABLE 1 AVERAGE SURFACE FORM DEVIATION (FLATNESS), AVERAGE WAVINESS (W_a) and AVERAGE WAVINESS SPACING (W_{sm}) MEASURED USING AN ALICONA INFINITEFOCUS

As is expected for a 'poli-lapping' finish quality, the procedure produces a very fine surface roughness value and the waviness is also very well controlled.

Examining the roughness more closely (Fig. 4), the random nature of the surface for a 100 μm square sample becomes apparent. Considering the aim of this work is to model leakage of only the roughness, then creating a geometric model of the whole surface of the seat and disc with roughness embedded into it, is not computationally feasible. The reason why a 100 μm square area is chosen for this study is to try and reduce any interference of the characteristics of waviness i.e. $100\mu\text{m} \ll W_{sm}$.

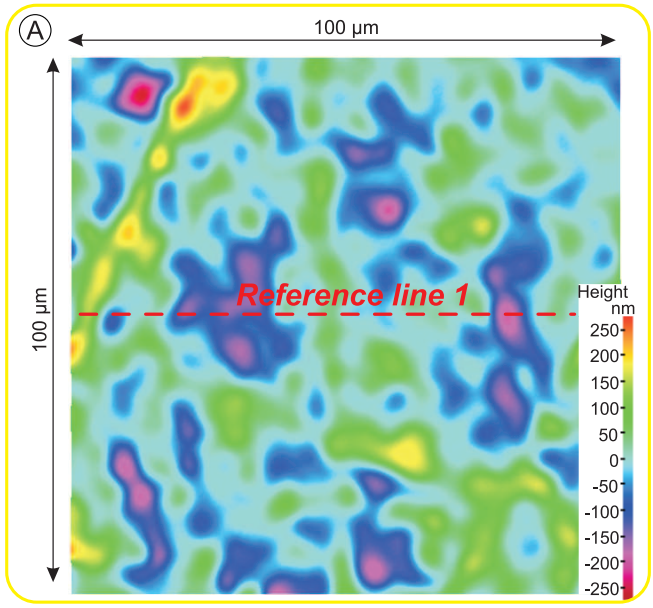

FIG. 4 100 μm BY 100 μm ACTUAL SCAN OF DISC USING THE ALICONA INFINITEFOCUS AT 50X OBJECTIVE MAGNIFICATION

CAD

A representative scaled model is used to capture the leakage via the surface roughness as shown in Fig. 5 coming in contact with a rigid-perfectly flat surface similar to the analysis conducted by Megalingam and Mayuram [9].

The original scan (Fig. 4) generates 1,048,576 nodes which if directly meshed in FEA or CFD it would be computationally challenging and expensive. The Alicona InfiniteFocus, works by measuring a specific area and then traversing to the adjacent area, until the full area of interest has been scanned. It then stitches all this data together generating a surface like that shown in Fig. 4. This method allows a high resolution of the surface to be generated as an 'STL' file format, however generating a lot of data. Instead the scan is discretized from 1,048,576 nodes to 1,000 nodes using 2 algorithms: the Poisson-disk distribution [10]; and the ball-pivoting algorithm [11]. Using these algorithms the discretisation yields an R_a value less than 5% of the original scan

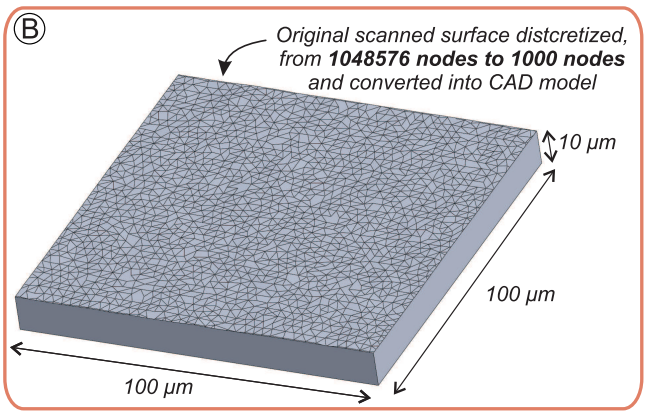

FIG. 5 100 μm BY 100 μm ACTUAL SCAN OF DISC CONVERTED INTO CAD FORMAT

(see Fig. 6). Both these algorithms can be found in freeware software such as MeshLab. This discretisation method would also be applicable to other optical-interferometry device measurements.

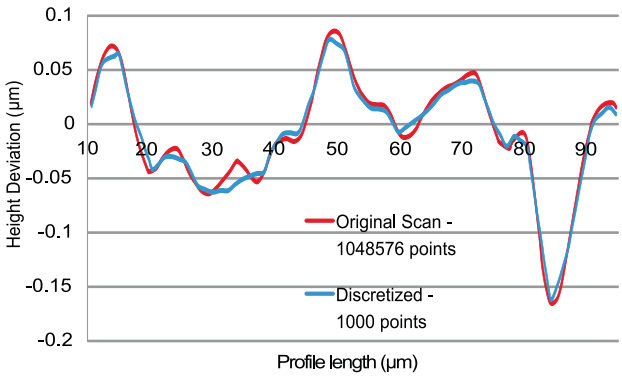

FIG. 6 REFERENCE LINE 1 OF ORIGINAL 100 μm BY 100 μm SCAN (FIG. 4) COMPARED TO DISCTRITIZED CAD MODEL OF SCAN

FEA

Using ANSYS® workbench (version 17), the geometric model is analysed using FEA to find the deformation of the contact surfaces due to the spring force in an elastic perfectly-plastic manner.

The disc is made of a Stellite Alloy while the seat is made of AISI 316N(L) steel. The perfectly flat rigid surface is assumed to be the disc and is made of SURF154 elements. The seat is modelled as AISI 316N(L) steel, elastic perfectly-plastic, and is predominantly made up of SOLID187 10-node elements, with the seat and disc contact surfaces associated with CONTA174 8-node and TARGE170 4-node quadratic elements associated with the rigid surface. The boundary conditions for the geometric model is displayed in Fig. 7.

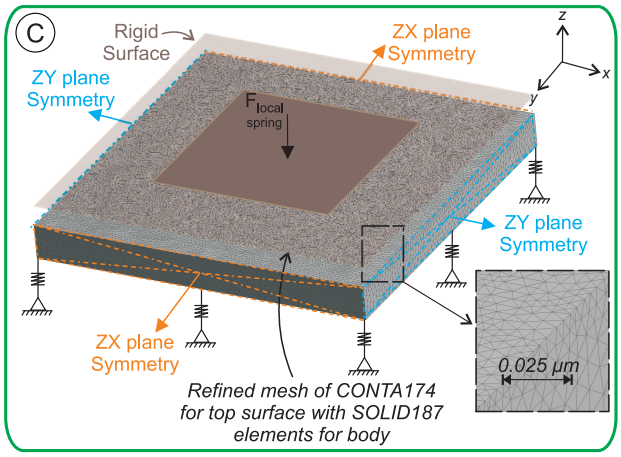

FIG. 7 ROUGHNESS FE MODEL WITH BOUNDARY CONDITIONS

The Roughness model is made up of 1,019,763 elements and 667,268 nodes. The mesh for the contact regions requires a high resolution to capture the micro scale contact deformation as shown in Fig. 7.

Symmetric boundary planes (ZX and ZY planes) are applied around the Roughness model to artificially mimic the whole surface. The bottom of the model has elastic support boundary conditions. This allows geometric simplification of the model while still allowing accurate simulation of the whole geometry.

The local spring force ($F_{local\ spring}$) in Fig. 7 is simply the fractional spring force based on the total seat and rigid surface contact area. As recommended in API 527 [3], when testing for leakage the spring force is increased to an amount which is capable of withstanding the P_{set}. The internal pressure (P_{in}) is then increased up to 90% of the P_{set}, then the leakage is measured. So to represent this in the FEA, the spring force ($F_{local\ spring}$) is applied to the rigid perfectly flat surface over 2 load steps (Fig. 8) using a static analysis. In the first load step the spring force is increased to a force representative of acting against P_{set}, which for this study is $F_{local\ spring} = P_{set}.A_{local}$. In the second load step the force is linearly reduced to 10% of the full spring force. Rather than modelling the P_{in} as a boundary condition, the internal pressure can be calculated using $P_{in} = F_{local\ spring}/A_{local}$, allowing artificial representation of the internal pressure up to the P_{set}, mimicking the behaviour which would be seen in reality.

Overall contact The FEA models are solved and at the P_{in} of interest the deformed gap between the seat and rigid surface requires exporting as a CAD file. The model is exported at the P_{in} of interest using an APDL script which builds a 'surface skin' over the deformed 3D model and converts into an 'IGES' file type. For more detailed information about this script, refer to reference [12].

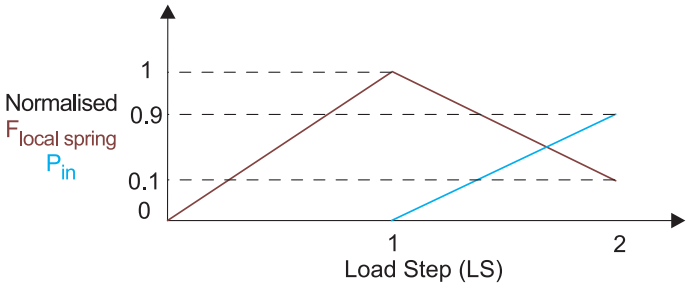

FIG. 8 SPRING FORCE APPLICATION WITH RESPECT TO LOAD STEP

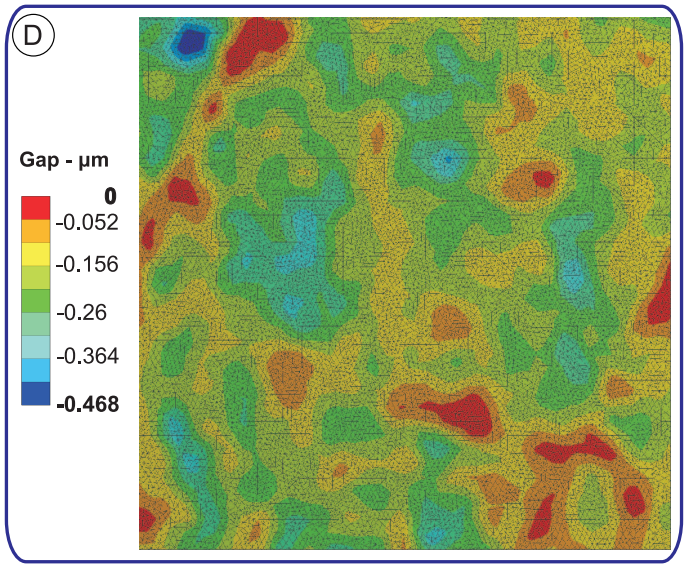

FIG. 9 D – OVERALL CONTACT GAP AT P_{int} 90% OF P_{set} = 0.5 MPa

CFD model

For the following CFD simulations, it is assumed that the fluid is an ideal gas (295K) of laminar air flow solved using the Navier-Stokes equations. The wall boundary conditions (i.e. top and bottom of channel) has a low pressure boundary slip condition applied which allows the Maxwell's model for velocity slip and temperature change to be considered ($0.01 < Kn < 0.1$) [13]. The inlet boundary condition is set to P_{in} and the outlet is set to 0 MPa.

To find the leakage of the fluid through the deformed gap due to the roughness, a Global-to-Local analysis is required (see Fig. 10). The Global Channel spans from the inner to the outer radius of the Seat ($L = R_{out} - R_{in}$), with the last 100 μm of the channel length being associated with the local model. The Global Channel height is the average gap height (found via section *G - Overall Gap/Contact* (Fig. 9 Roughness FEA Model)).

The global model has either side of the channel set as a symmetric boundary condition, and the top and the bottom of the channel assumed to be a wall with the same Maxwell slip model applied.

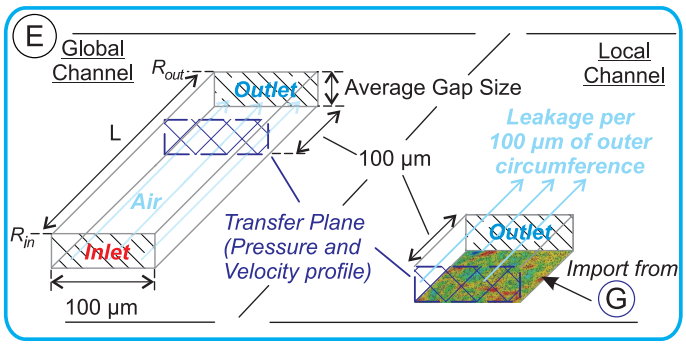

FIG. 10 GLOBAL-TO-LOCAL MODEL TO FIND LOCAL LEAKAGE ATTRIBUTED TO ROUGHNESS

Once the Global Channel CFD is solved, 100 μm back from the outlet of the channel length, the velocity and temperature profiles are extracted and used as inlet conditions for the local model.

The local model is the deformed gap imported from the Roughness FEA model (Fig. 9) and meshed using tetrahedral elements (2,064,769 nodes and 10,284,328 nodes). Solving this CFD model results in leakage attributed to the roughness per 100 μm of the outer circumference.

RESULTS AND DISCUSSION

The following results are conducted for the spring-loaded for a $P_{set} = 0.5$ MPa.

FEA – von Mises Stress

Fig. 11 shows the von Mises stress plot obtained across the model when the full spring force is applied at the end of the first load step.

The roughness model (Fig. 11) yields at the higher peak points with a stress distribution across the surface. This is expected considering the peak points would come in contact first. The plastic yielding does not extend a great deal due to the force not being high enough to do so. However, it is noted that the interaction of the asperities at the surface level have a certain influence on evolving the contact stress at the base. This evolving contact at the base has been noted in experiments conducted by Uppal and Probert [14] who studied the deformation effects on single and multiple asperities on metal surfaces.

CFD – Leakage

The FEA-CFD numerical method was solved for a P_{in} of 75%-99.5% for a P_{set} = 0.5 MPa. The results are displayed in Fig. 12.

The results show a linear change in leakage up between 75% and 90% of P_{set}, with a larger gradient change between 95% and 99.5% of P_{set}. The linear change in leakage is due to the FEA roughness model deformation, were the model will deform due to the elastic boundary condition and also due to the elastic

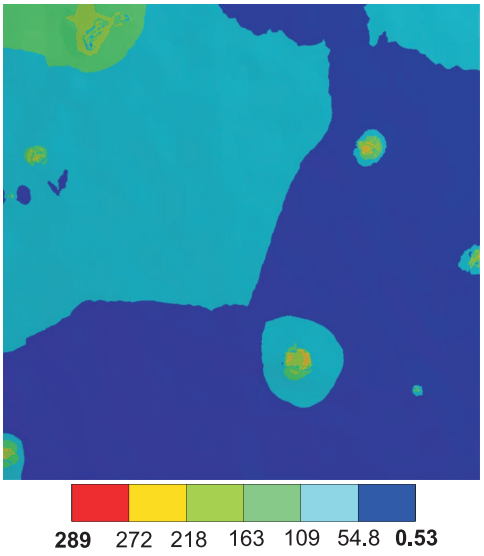

FIG. 11 VON-MISES STRESS PLOT OF ROUGHNESS MODEL IN MPA

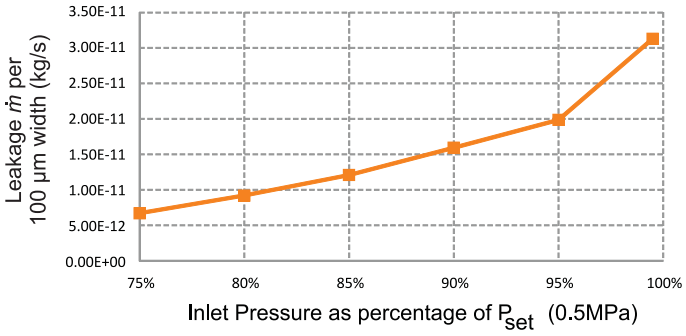

FIG. 12 LEAKAGE OF VALVE PER 100 μm WIDTH, BASED ON THE SURFACE ROUGHNESS SCAN

perfectly-plastic condition of the material. As the inlet pressure increases between 75% and 90%, the model will begin to return to its original position due to the elastic boundary condition. Between 95% and 99.5%, the asperities will return to there original position, while the plastically deformed zones will remain deformed causing a sudden gradient change in leakage between 95% and 99.5% inlet pressure.

According to API 527 [3] at 90% of the P_{set} this particular valve has a maximum leak rate of 20 bubbles/min. Based on the roughness leakage result at 90% P_{set} of 0.5 MPa (Fig. 12), the outer circumference of the seat and a perfect sphere measuring 7.9 mm (this is based on the outlet pipe diameter specified for measuring leakage using the API 527), the leakage rate for the valve would be 4.9 bubbles/min. This is less than the API527 maximum rate specified therefore an acceptable leakage rate.

Surface form and waviness

From Table 1, it was found that both the seat and disc show a greater waviness and form magnitude than the roughness. What is apparent is that the surface form will produce the greatest gap when both surfaces are in contact and therefore be the greatest contributor to leakage. The roughness will contribute the least leakage since it would generate the smallest gap between the contacting faces. Therefore, this roughness model would work well as a sub-model of a larger model which incorporates the form and waviness surface characteristics.

CONCLUSIONS

A numerical methodology using an actual scan 100 μm x 100 μm of the disc used in a spring-loaded PRV has been incorporated into a FEA-CFD solver. The scan produced using an optical interferometry device was successfully discretized within 5% of the original scan into a representative CAD model. FEA of the model resulted in obtaining the deformation behaviour of the asperities due to an applied spring force. Using a global-to-local CFD analysis, the change in leakage of the PRV based on the FE deformed elastic perfectly-plastic asperities up to a $Pset = 0.5$ MPa was found.

ACKNOWLEDGMENT

There are many people without whom this research project could not have been possible. The authors would like to thank:

- The individuals whose research has been mentioned in this paper, since without their great work, this work would have not come about;
- The WEIR group and the WEIR Advanced Research Center (WARC) in particular, Alan Bickley, Allan Stewart, Stéphane Carrier and Fabrice Courdavault;
- Brian Kyte (Sales Director at Alicona UK) for the help in getting access to the Alicona InfiniteFocus and addressing technical matters;
- Liza Hall (University of Strathclyde, Advanced Forming and Research Centre, Metrology) for allowing to use the Alicona InfiniteFocus and addressing technical matters;
- Rong Su and Wahyudin Syam (University of Nottingham, Institute for Advanced Manufacturing) for allowing to use the Alicona InfiniteFocus and addressing technical matters;
- Ricky Martin at ARCHIE-WEST (University of Strathclyde) - Results were obtained using the EPSRC funded ARCHIE-WeSt High Performance Computer (www.archie-west.ac.uk) EPSRC grant no. EP/K000586/1.

REFERENCES

[1] Ralph A. Dodds, I., 2013. SRV-3B safety relief valve declared inoperable due to leakage and setpoint drift. Report no. 2013-002-00, U.S. Nuclear Regulatory Commission, Attn: Document Control Desk, Washington, D.C. 20555, Mar.

[2] Watanabe, N., 2008. "Trend analysis of incidents involving setpoint drift in safety or safety/relief valves at US LWRs". *Nippon Genshiryoku Gakkai Wabun Ronbunshi,* ***7***(1), pp. 74–84.

[3] API, 2014. *Seat Tightness of Pressure Relief Valves*. No. 527 in API Standard. American Petroleum Institute, Washington, USA.

[4] BSI, 2013. *Safety devices for protection against excessive pressure. Safety valves*. No. BS EN ISO 4126-1:2013 in British Standard. The British Standards Institution, London, UK.

[5] ASME, 2014. *Pressure Relief Devices – Performance Test Codes*. No. ASME PTC 25-2014 in an American National Standard. The American Society of Mechanical Engineers, New York, USA.

[6] Burmeister, L. C., Loser, J. B., and Sneegas, E. C., 1967. Advanced valve technology – Revised and enlarged edition. Technology Survey no. NASA SP-5019, Midwest Research Institute, NASA, Washington, D.C., USA.

[7] BHR Group Ltd., 2000. Valve stem leak – tightness test methodologies. Summary report no. CR1234, European Commission, British Hydromechanics Research Group Ltd., Cranfield, UK, Oct.

[8] Anwar, A. A., Gorash, Y., and Dempster, W., 2016. "Application of multi-scale approaches to the investigation of sealing surface deformation for the improvement of leak tightness in pressure relief valves". In *Advanced Methods of Continuum Mechanics for Materials and Structures*, K. Naumenko and M. Aßmus, eds. Springer, Singapore, pp. 493–522.

[9] Megalingam, A., and Mayuram, M., 2012. "Elastic-plastic contact analysis of single layer solid rough surface model using FEM". *Int. J. of Mechanical, Aerospace, Industrial, Mechatronic and Manufacturing Engineering,* ***6***(1), pp. 133–137.

[10] Corsini, M., Cignoni, P., and Scopigno, R., 2012. "Efficient and flexible sampling with blue noise properties of triangular meshes". *IEEE Transaction on Visualization and Computer Graphics,* ***18***(6), pp. 914–924.

[11] Bernardini, F., Mittleman, J., Rushmeier, H., Silva, C., and Taubin, G., 1999. "The ball-pivoting algorithm for surface reconstruction". *IEEE Transactions on Visualization and Computer Graphics,* ***5***(4), Oct., pp. 349–359.

[12] Group, S., 2016. Export the deformed geometry shape from a model., Oct. See also URL https://www.simutechgroup.com/tips-and-tricks/fea-articles/225-export-the-deformed-geometry-shape-from-ansys-model.

[13] ANSYS® Help, 2015. *Fluent // Theory Guide // 7. Species Transport and Finite-Rate Chemistry // 7.2.3. Slip Boundary Formulation for Low-Pressure Gas Systems*, Academic Research 16.1.0 ed. ANSYS, Inc., Canonsburg (PA), USA.

[14] Uppal, A., and Probert, S., 1972. "Deformation of single and multiple asperities on metal surfaces". *Wear,* ***20***(3), pp. 381–400.